

# Luteolin attenuates angiotensin II-induced renal damage in apolipoprotein E-deficient mice

YING-SHU LIU<sup>1</sup>, QIN YANG<sup>2</sup>, SHEN LI<sup>1</sup>, LAN LUO<sup>1</sup>, HONG-YANG LIU<sup>3</sup>,  
XIN-YU LI<sup>1</sup> and ZHENG-NAN GAO<sup>1</sup>

<sup>1</sup>Department of Endocrinology, Dalian Municipal Central Hospital Affiliated of Dalian Medical University; <sup>2</sup>Department of Internal Medicine, The Affiliated Zhong Shan Hospital of Dalian University; <sup>3</sup>Department of Heart Intensive Care Unit, The First Affiliated Hospital of Dalian Medical University, Dalian, Liaodong 116011, P.R. China

Received June 4, 2020; Accepted November 26, 2020

DOI: 10.3892/mmr.2020.11796

**Abstract.** Renal damage is a common and severe condition encountered in the clinic. Luteolin (Lut) exhibits anti-inflammatory, anti-fibrotic and anti-apoptotic effects. Thus, the present study aimed to investigate the pharmacological effects of Lut on angiotensin II (AngII)-induced renal damage in apolipoprotein E-deficient (ApoE<sup>-/-</sup>) mice. Male ApoE<sup>-/-</sup> mice (age, 8 weeks) were randomly divided into the following three groups: i) Control group (n=6); ii) AngII group (n=6); and iii) AngII + Lut group (n=6). Lut was administered by gavage (100 mg/kg/d). ApoE<sup>-/-</sup> mice were implanted with Alzet osmotic minipumps, filled with either saline vehicle or AngII solution for a maximum period of 4 weeks. After 4 weeks, metabolic characteristics were measured and the histopathological alterations in the kidney tissue were observed. The metabolic characteristics of blood creatinine (CRE) levels were lower in the AngII + Lut group compared with in the AngII group. The expression levels of collagen I and III were lower in the kidney tissues of the AngII + Lut group compared with the corresponding tissues of the AngII group. The gene expression levels of IL-1 $\beta$ , IL-6, TNF- $\alpha$  and IL-10 were also suppressed in the kidney tissues of the AngII + Lut group compared with those in the corresponding tissues of the AngII group. Furthermore, the AngII + Lut group exhibited markedly increased LC3 protein expression and notably decreased p62 protein expression in the kidney tissues compared with the expression levels in the AngII group. The data demonstrated that Lut attenuated AngII-induced collagen deposition and inflammation, while inducing autophagy. Collectively, the results suggested that Lut treatment exhibited an exerted effect on AngII-induced renal injury in ApoE<sup>-/-</sup> mice.

## Introduction

Renal damage is common in the end-stage of numerous types of disease, such as diabetic nephropathy and hypertension nephropathy (1,2). Therefore, the identification of effective methods that can attenuate this condition is a major focus of investigations. Angiotensin II (AngII) exerts a vasoconstrictor effect, which may contribute to the onset and progression of renal damage (3,4). In addition, AngII may directly accelerate renal damage by recruiting inflammatory cells and by sustaining cell proliferation and fibrosis (5,6). Several studies have revealed that AngII induces pathological responses in ischemia-reperfusion (I/R) injury, exhibiting tubular epithelial cell necrosis, cellular failure and increased permeability (7,8). Moreover, accumulating evidence has suggested that autophagy serves an important role in renal damage (9,10). However, whether the induction of autophagy contributes to cell survival or cell death remains unclear.

Luteolin (Lut; 3',4',5,7-tetrahydroxyflavone) is widely found in vegetables, fruits and plants. For instance, dietary products, such as carrots, cabbage, celery, olive oil, peppermint and apples are good sources of Lut (11). The molecular formula of Lut is C<sub>15</sub>H<sub>10</sub>O<sub>6</sub> and its structure is presented in Fig. 1 (12,13). It has been reported that a variety of traditional Chinese medicines, such as *Chrysanthemum*, *Herba Ajugae* and honey-suckle contain excess amounts of Lut (14). Accumulating evidence has suggested that Lut exhibits anti-inflammatory, anti-fibrotic and anti-tumor effects (14-17). Previous studies have also reported that Lut can protect against renal I/R injury, lipopolysaccharide (LPS)-induced acute renal injury and cisplatin-induced nephrotoxicity (13,14,18,19). However, to the best of our knowledge, the role of Lut treatment on AngII-induced renal damage in apolipoprotein E-deficient (ApoE<sup>-/-</sup>) mice has not been previously examined. Therefore, in the present study, the effects of Lut were investigated in AngII-induced renal damage in ApoE<sup>-/-</sup> mice.

## Materials and methods

**Animal studies.** According to the previous research, ApoE<sup>-/-</sup> mice were selected as the experimental animals (20,21).

---

*Correspondence to:* Professor Zheng-Nan Gao, Department of Endocrinology, Dalian Municipal Central Hospital Affiliated of Dalian Medical University, 42 Xuegong Street, Dalian, Liaodong 116011, P.R. China  
E-mail: gao2008@163.com

**Key words:** angiotensin II, renal damage, apolipoprotein E-deficient mice, luteolin

ApoE<sup>-/-</sup> mice (n=18) were provided from Beijing Vital River Lab Animal Technology Co., Ltd. All the ApoE<sup>-/-</sup> mice had free access to feed on a conventional and standard mice chow diet with clean water, and were caged under constant conditions, including a 12-h dark/light cycle, and 40-60% humidity at 24°C. At 8 weeks of age, male mice (23.7±0.9 g) were randomly divided into three groups as follows: i) Control group (n=6); ii) AngII group (n=6); and iii) AngII + Lut group (n=6). Lut (cat. no. MB2172; Dalian Meilun Biology Technology Co., Ltd.) was administered by gavage (100 mg/kg/d) (8,22). ApoE<sup>-/-</sup> mice were implanted with Alzet osmotic minipumps (Model2004; Durect Corporation), filled with either saline vehicle or AngII solution (1,000 ng/kg/min) for a maximum period of 4 weeks (23,24). Each group of mice was subjected to its respective treatment for 4 weeks. The health and behaviour of the mice were monitored every day, and after 4 weeks, all mice were alive. The mice were anesthetized with a high dose of pentobarbital (100 mg/kg, intraperitoneally), blood samples (0.5-0.6 ml) were collected from the abdominal aorta, and then the mice were euthanized via cervical dislocation. The cessation of respiration and heartbeat indicated the death of the mice. Kidney tissues were harvested for further analysis. Serum samples were subsequently stored at -80°C until further use. The kidneys were frozen in liquid nitrogen for mRNA, histopathological and immunoblotting analyses. The current study was performed in accordance with the Guide for the Care and Use of Laboratory Animals (National Institutes of Health) (25) and was approved by the Ethics Committee of Dalian Municipal Central Hospital Affiliated of Dalian Medical University.

**Biochemical measurements.** Serum concentrations of creatinine (CRE) were measured using an ELISA kit (cat. no. C011-2-1; Nanjing Jiancheng Bioengineering Institute), according to the manufacturer's protocols.

**Hematoxylin and eosin (H&E) staining.** The kidney tissues at room temperature were fixed in 10% buffered formalin solution and subsequently dehydrated in 75% ethanol overnight, followed by paraffin embedding. Serial sections (thickness, 4 µm) were subjected to hematoxylin staining for 15 min and eosin staining for 5 min at room temperature to assess the pathological changes. Renal injury scores were determined by two blinded researchers according to the extent of the kidney injury, as previously described (13,26). The score grading was mainly based on the presence or absence of hemorrhage, tubular cell necrosis, tubular dilatation and cytoplasmic vacuole formation. The grading system was scored as follows: i) 0, normal kidney; ii) 1, 0-5% injury (minimal damage); iii) 2, 5-25% injury (mild damage); iv) 3, 25-75% injury (moderate damage); and v) 4, 75-100% injury (severe damage). All sections were examined using a BX40 upright light microscope (Olympus BX43; Olympus Corporation; scale bar, 100 µm).

**Masson's trichrome staining.** Kidney tissues from each group were at room temperature stored in 10% formalin, dehydrated in an ascending series of alcohol (75, 85, 90 and 100%; 5 min each) and finally embedded in paraffin wax. Then, 4 µm-thick paraffin sections were sliced from these paraffin-embedded

Table I. Primer oligonucleotide sequences.

Gene	Primer sequences
IL-1β	F: 5'-TGCCACCTTTTGACAGTGAT-3' R: 5'-TGTGCTGCTGCGAGATTTGA-3'
IL-6	F: 5'-TACCAGTTGCCCTTCTTGGGACTGA-3' R: 5'-TAAGCCTCCGACTTGTGAAGTGGT-3'
TNF-α	F: 5'-TCTCATGCACCACCATCAAGGACT-3' R: 5'-ACCACTCTCCCTTTGCAGAACTCA-3'
β-actin	F: 5'-CGATGCCCTGAGGGTCTTT-3' R: 5'-TGGATGCCACAGGATTCCAT-3'

F, forward; R, reverse.

tissue blocks. The tissue sections were subsequently deparaffinized via immersion in xylene (3 times; 5 min each) and rehydrated using a descending series of alcohol (100, 90, 85 and 75%; 5 min each). Biopsy samples were stained at room temperature using Masson's trichrome stain to investigate changes in the kidney morphology and fibrosis. Blue staining represented collagen accumulation. All sections were examined using a BX40 upright light microscope (Olympus BX43; Olympus Corporation).

**RNA isolation and reverse transcription-quantitative PCR (RT-qPCR).** Total RNA was extracted with *TransZol* Up Plus RNA Kit (cat. no. ER501-01; TransGen Biotech Co., Ltd.), and then RNA concentration and purity were measured using ISOGEN (cat. no. 317-02503; Nippon Gene Co., Ltd.). cDNA was synthesized using a first-strand cDNA synthesis kit (SuperScript VILO cDNA synthesis kit; Thermo Fisher Scientific, Inc.), according to the manufacturer's protocols. RT-qPCR was performed using fluorescent SYBR-Green technology (Light Cycler; Roche Molecular Diagnostics). The following thermocycling conditions were used for qPCR: Initial denaturation at 95°C for 20 sec; followed by 45 cycles of 60°C for 30 sec and 72°C for 60 sec; and a cooling step at 4°C. The relative expression of the target genes was normalized to that of β-actin. The relative gene expression was determined using the 2<sup>-ΔΔCq</sup> method (27). The primer sequences used for amplification are listed in Table I.

**Western blot analysis.** Total protein was extracted from kidney tissues using RIPA lysis buffer (cat. no. R0020; Beijing Solarbio Science & Technology Co., Ltd.), according to the manufacturer's protocols. Kidney tissue total protein concentrations were determined using a BCA Protein assay reagent kit (cat. no. DQ111-01; Beijing Transgen Biotech Co., Ltd.). Protein samples (30 µg per lane) were separated by SDS-PAGE on 10-15% gels, and were subsequently transferred to PVDF membranes. Subsequently, membranes were blocked in Tris-buffered saline with 0.1% Tween-20 (TBST) containing 5% skimmed milk, and then incubated at room temperature for 2 h. The membranes were then incubated with primary antibody diluent (cat. no. P0023A; Beyotime Institute of Biotechnology) and lightly shaken overnight at 4°C. Primary

Table II. Metabolic data from the three groups after 4 weeks of treatment.

Groups	Control (n=6)	AngII (n=6)	AngII + Lut (n=6)
Body weight, g	26.12±2.60	25.33±1.06	26.43±0.81
Kidney/body weight ratio, mg/g	6.80±1.45	6.23±0.54	6.31±0.22
Creatinine, $\mu\text{mol/l}$	31.24±3.73 <sup>a</sup>	93.21±6.61	36.86±4.53 <sup>a</sup>

Data are presented as the mean  $\pm$  SEM; n=6 per group. <sup>a</sup>P<0.05 vs. AngII group. AngII, angiotensin II; Lut, luteolin.

antibody rabbit against collagen I (cat. no. 14695-1-AP; 1:1,000; ProteinTech Group, Inc.), collagen III (cat. no. 22734-1-AP; 1:1,000; ProteinTech Group, Inc.), microtubule associated protein 1 light chain 3 $\alpha$  (LC3; cat. no. 14600-1-AP; 1:1,000; ProteinTech Group, Inc.), p62 (cat. no. 55274-1-AP; 1:1,000; ProteinTech Group, Inc.) and  $\beta$ -actin (cat. no. 20536-1-AP; 1:1,000; ProteinTech Group, Inc.) was performed. Briefly, the kidney tissues were harvested, and the protein extracts were prepared according to established methods. The extracts were separated via SDS-PAGE (8-15%) and transferred to a PVDF membrane (EMD Millipore). The membranes were blocked overnight with 5% milk blocking reagent at 4°C. The proteins were visualized by the addition of the respective antibodies, followed by the incubation with species-specific peroxidase-labeled secondary antibodies (cat. no. 7074; anti-rabbit IgG; 1:2,000; Cell Signaling Technology, Inc.) for 1 h.  $\beta$ -actin was used as a control of the equal protein loading. The protein levels were expressed as protein/ $\beta$ -actin ratios to minimize loading. Chemiluminescence reagent (ProteinTech Group, Inc.) was used to visualize bands. This analysis was performed three times independently. The intensity of the bands was semi-quantified using ImageJ software version 1.8.0 (National Institutes of Health).

**Immunohistochemical analysis.** Kidney tissues were fixed in 10% buffered formalin solution for 30 min at room temperature and dehydrated in 75% ethanol overnight, followed by paraffin embedding. Immunohistochemical analysis was performed using the SP-9001 SPlink Detection kits (OriGene Technologies, Inc.), according to the manufacturers' instructions. Paraffin-embedded sections (4  $\mu\text{m}$ ) were deparaffinized with xylene and subsequently rehydrated in a descending series of ethanol washes (100, 90, 85 and 75%; 5 min each). The sections were treated for 15 min at 98°C with 3% H<sub>2</sub>O<sub>2</sub> in methanol to inactivate the endogenous peroxidase activity and were subsequently incubated at room temperature for 1 h with primary antibodies rabbit against collagen I (cat. no. 14695-1-AP; 1:200; ProteinTech Group, Inc.), collagen III (cat. no. 22734-1-AP; 1:200; ProteinTech Group, Inc.), LC3 (cat. no. 14600-1-AP; 1:200; ProteinTech Group, Inc.) and p62 (cat. no. 55274-1-AP; 1:200; ProteinTech Group, Inc.). The secondary antibody from SPlink Detection kits (OriGene Technologies, Inc.) was incubated with the tissue for 30 min at room temperature. All sections were examined using a BX40 upright light microscope (Olympus BX43; Olympus Corporation). For each staining, 3x7 sections (6 mice) per group were analyzed and the representative images were presented. All image analyses were performed by a blinded reviewer.

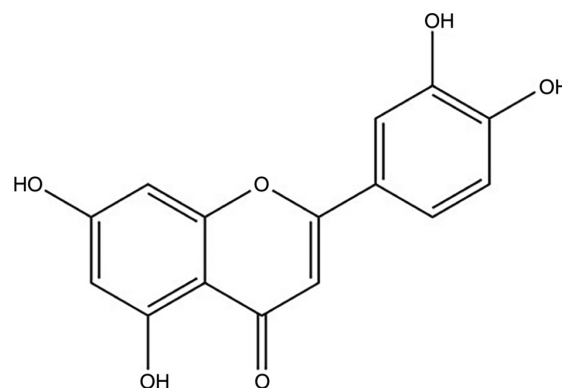


Figure 1. Basic structure of luteolin (3',4',5',7'-tetrahydroxyflavone).

**Statistical analysis.** All data are presented as the mean  $\pm$  SEM, and all experiments were repeated at least three times. SPSS version 19.0 software (IBM Corp.) was used for statistical analysis. The Kolmogorov-Smirnov test was used to detect the normality of all data. Inter-group variation was measured using a one-way ANOVA, followed by individual comparisons with a Tukey's tests. P<0.05 was considered to indicate a statistically significant difference.

## Results

**Lut increases CRE concentration and improves renal function.** The kidney/body weight ratio did not differ among the three groups. The metabolic characteristics of ApoE<sup>-/-</sup> mice from the three groups following 4 weeks of treatment are presented in Table II. The CRE levels in the AngII-induced ApoE<sup>-/-</sup> mice were increased by 198% compared with those of the control group (93.21±6.61 vs. 31.24±3.73  $\mu\text{mol/l}$ ; P<0.05), indicating a reduction of renal function. The CRE levels of the AngII + Lut group were markedly decreased by 60.5% following the treatment of the mice with Lut compared with those in the AngII group (36.86±4.53 vs. 93.21±6.61  $\mu\text{mol/l}$ ; P<0.05). No difference was noted between the AngII + Lut and control groups.

**Lut improves the histopathological characteristics of the AngII-treated kidney tissues.** To evaluate the histopathological damage in the kidney tissue, H&E staining was performed (Fig. 2A). The AngII + Lut group had markedly reduced inflammatory cell infiltration in the kidney tissues compared with that observed in the AngII group. These results suggested that Lut decreased inflammatory cell infiltration in the AngII-induced renal damage of ApoE<sup>-/-</sup> mice. Renal

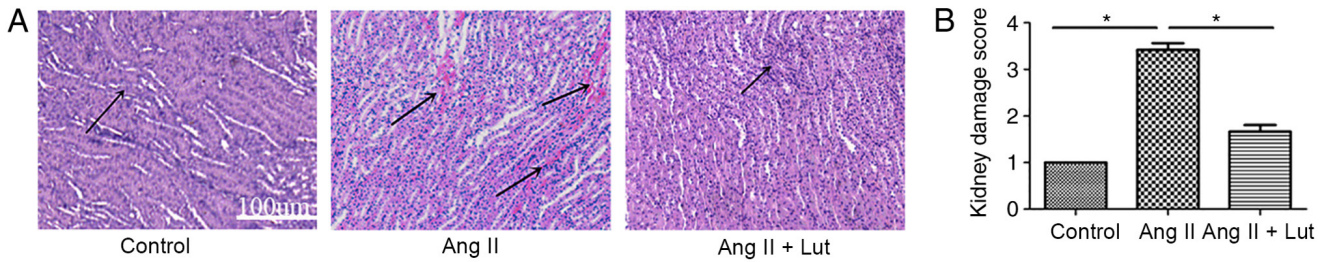


Figure 2. Effect of Lut on AngII-induced renal damage as presented by hematoxylin and eosin staining. Arrows indicate inflammatory infiltration. (A) Luteolin could attenuate inflammatory cells infiltration in AngII + Lut group compared with the AngII group of ApoE<sup>-/-</sup> mice. Scale bar, 100  $\mu$ m. (B) Kidney damage scores are expressed as mean  $\pm$  SEM. Semi-quantitative injury scores range from 0 to 4 [0, normal kidney; 1, minimal damage (0-5% injury); 2, mild damage (5-25% injury); 3, moderate damage (25-75% injury); and 4, severe damage (75-100% injury)]. \*P<0.05. Lut, luteolin; AngII, angiotensin II; ApoE<sup>-/-</sup>, apolipoprotein E-deficient.

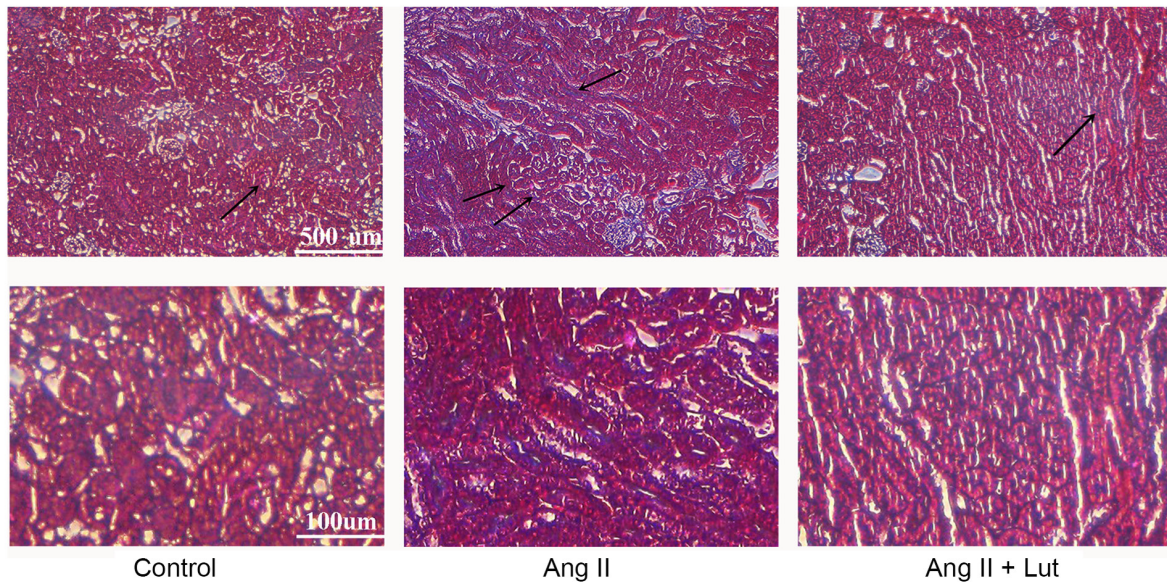


Figure 3. Effect of Lut on AngII-induced kidney tissue fibrosis. Fibrosis was evaluated using Masson's trichrome staining, where kidney tissues are stained red and collagenous fibres are stained blue. The arrows indicate fibrosis. Scale bar, 100 and 500  $\mu$ m. Lut, luteolin; AngII, angiotensin II.

injury scoring (Fig. 2B) demonstrated that Lut treatment could significantly decrease renal injury caused by AngII in mice, which was consistent with the H&E results.

*Lut inhibits collagen deposition in AngII-treated kidney tissues.* Masson's trichrome staining indicated that collagen deposition was significantly increased in the interstitium and the perivascular and subvascular areas, suggesting that AngII induced renal interstitial fibrosis. Lut treatment markedly attenuated the AngII-induced collagen deposition (Fig. 3). Taken together, these data demonstrated that Lut attenuated renal fibrosis in AngII-induced kidney tissues.

*Lut inhibits collagen I and III protein expression levels in AngII-treated kidney tissues.* Collagen I and collagen III (Fig. 4A) immunostaining was performed. The AngII + Lut group exhibited markedly decreased collagen I and III expression levels in the kidney tissues compared with those observed in the AngII group (Fig. 4B). The expression levels of collagen I and III proteins in the kidney tissues were also determined via western blotting (Fig. 4C). The results indicated that the protein expression levels of collagen I and III in the mice of the AngII + Lut group were

significantly suppressed compared with those in the AngII group (Fig. 4D).

*Lut attenuates autophagy in AngII-treated kidney tissues.* To evaluate the expression levels of LC3 and p62 in kidney tissues, LC3 and p62 (Fig. 5A) immunostaining was performed. The AngII + Lut group exhibited markedly increased LC3 and decreased p62 expression levels in the kidney tissues compared with those observed in the AngII group (Fig. 5B). The protein expression levels of LC3 and p62 in the kidney tissues were also determined via western blotting (Fig. 5C). The results demonstrated that LC3 protein expression in the AngII + Lut group was significantly increased compared with that in the AngII group, whereas p62 protein expression in the AngII + Lut group was significantly decreased compared with those in the AngII group (Fig. 5D). These results indicated that Lut increased LC3 expression and decreased p62 expression in ApoE<sup>-/-</sup> mice with AngII-induced renal damage.

*Lut inhibits pro-inflammatory cytokine expression in AngII-treated kidney tissues.* The expression levels of IL-1 $\beta$ , IL-6, TNF- $\alpha$  and IL-10 were measured using RT-qPCR (Fig. 6). The expression levels of IL-1 $\beta$ , IL-6 and TNF- $\alpha$  were

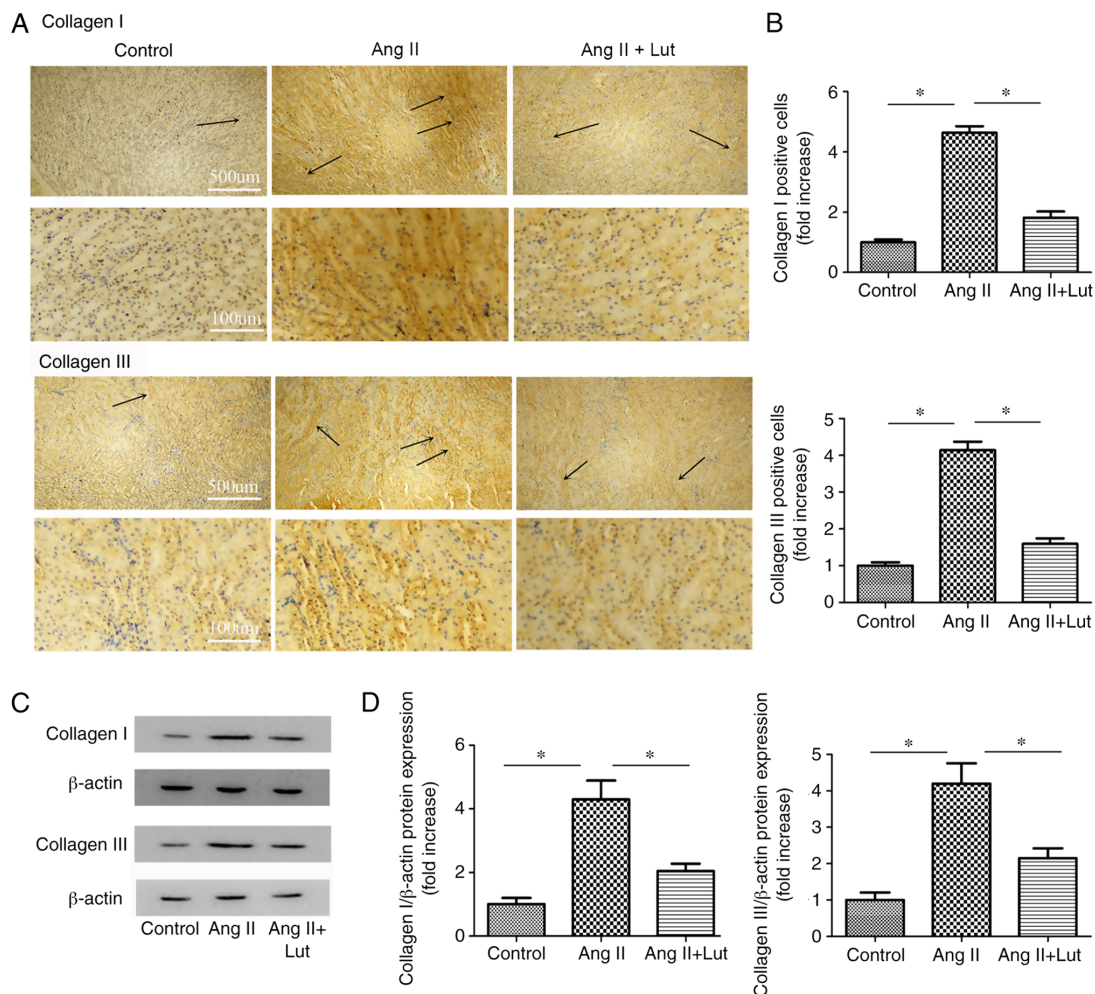


Figure 4. Protein expression levels of collagen I and collagen III in kidney tissues as determined via western blotting. (A) Representative immunohistochemistry for collagen I and collagen III in kidney tissue. Arrows indicate positively collagen I and collagen III stained cells. Scale bar, 100 and 500  $\mu\text{m}$ . (B) Bar graph illustrating collagen I and collagen III positive cells. (C) Immunoblotting for collagen I and collagen III in kidney tissues. (D) Semi-quantification of collagen I and collagen III protein expression levels. Data are presented as the mean  $\pm$  SEM; n=3 per group. \*P<0.05. Lut, luteolin; AngII, angiotensin II.

significantly elevated in the AngII group compared with those of the control group. However, Lut treatment decreased significantly the expression levels of IL-1 $\beta$ , IL-6 and TNF- $\alpha$  compared with the AngII group. The expression levels of IL-10 did not show these changes.

## Discussion

In the present study, the protective effects of Lut were examined using a model of AngII-induced nephropathy in ApoE<sup>-/-</sup> mice. The results suggested that Lut attenuated AngII-induced collagen deposition and inflammation. These processes were accompanied with the induction of autophagy.

The AngII group in ApoE<sup>-/-</sup> mice had a marked increase in CRE levels, whereas this parameter was notably decreased in the AngII + Lut group. No significant differences were identified between the AngII + Lut and control groups. This indicated that Lut attenuated impaired renal function. A number of studies have reported similar results. For instance, Xin *et al* (14) revealed that CRE levels were increased 2.10-fold in LPS-treated mice compared with those of normal mice. In addition, CRE levels were significantly decreased by 38.5% following Lut treatment compared with the LPS-treated

mice (14). However, the Lut group did not differ with regard to renal function indices compared with the control group. Hong *et al* (13) also demonstrated that Lut treatment resulted in significantly reduced serum levels of CRE in I/R mice.

Collagen deposition was increased significantly in the interstitium and the perivascular and subvascular areas of AngII-induced ApoE<sup>-/-</sup> mice, as determined via Masson's trichrome staining. Lut treatment significantly attenuated the AngII-induced collagen deposition. This observation was further confirmed by protein expression studies. The protective effects of Lut were mediated by a reduction of the AngII-induced increase in collagen I and III proteins. These results indicated that Lut exhibited a therapeutic effect on kidney fibrosis induced by AngII. Moreover, several studies have reported that Lut decreases the extent of collagen deposition and fibrosis in other organs, such as lung, liver and myocardium (12,28,29). Moreover, Domitrović *et al* (28) reported that the protective effect of Lut on CCl<sub>4</sub>-induced liver fibrosis was mediated by promoting extracellular matrix degradation and the stimulation of hepatic regenerative capability.

It has been shown that inflammatory cell infiltration is a key factor in renal damage (30). The present study demonstrated

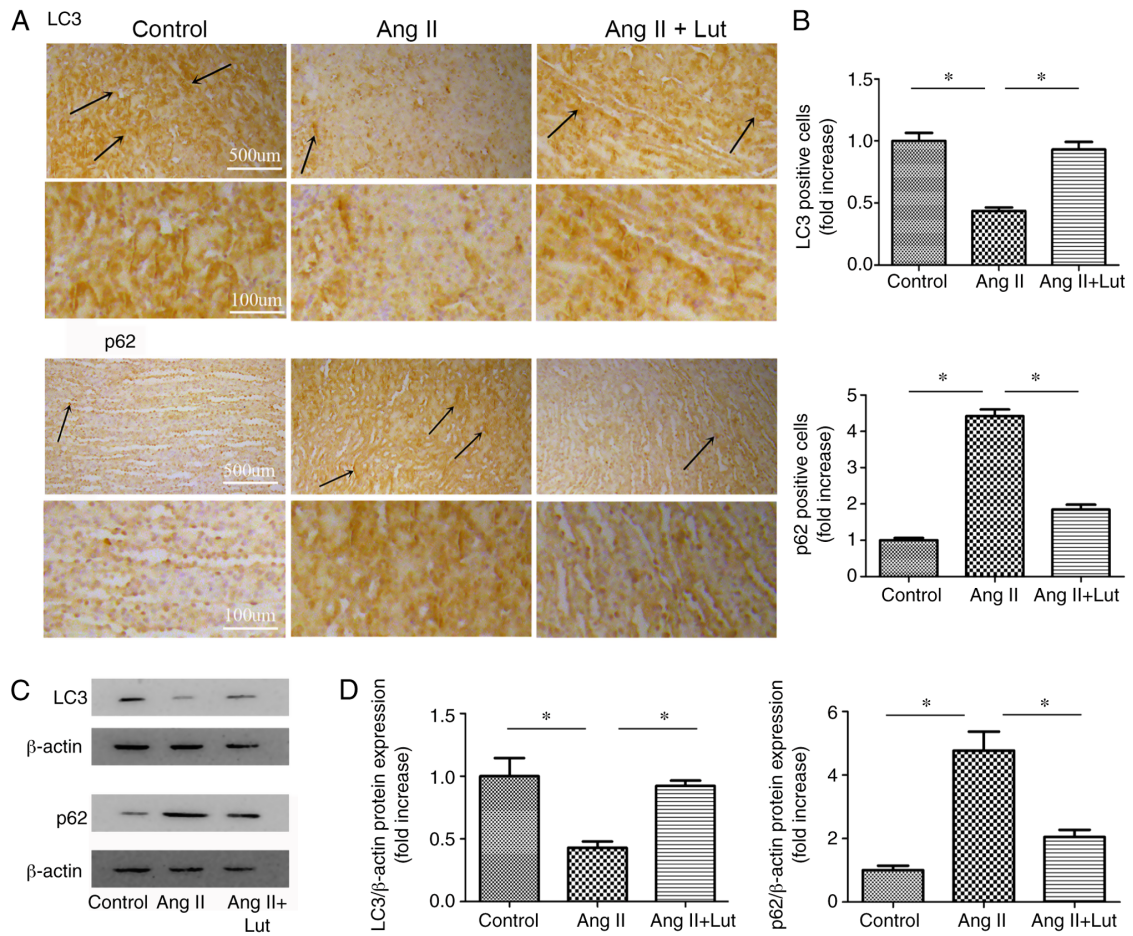


Figure 5. LC3 and p62 expression levels in kidney tissue from the three groups after 4 weeks of treatment. (A) Representative immunohistochemistry for LC3 and p62 in kidney tissue. Arrows indicate positively LC3 and p62 stained cells. Scale bar, 100 and 500  $\mu$ m. (B) Bar graph of LC3 and p62 positive cells. (C) Immunoblotting for LC3 and p62 in kidney tissues. (D) Semi-quantification of LC3 and p62 protein expression levels. Data are presented as the mean  $\pm$  SEM; n=3 per group. \*P<0.05. Lut, luteolin; AngII, angiotensin II; LC3, microtubule associated protein 1 light chain 3 $\alpha$ .

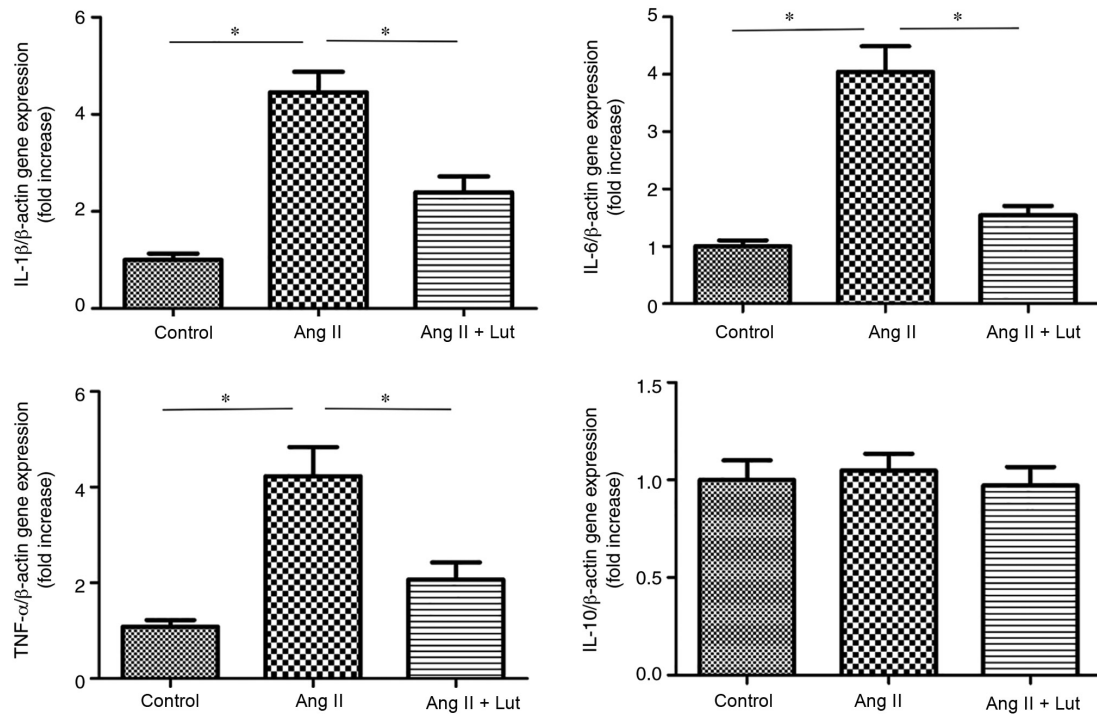


Figure 6. Expression levels of pro-inflammatory genes in AngII-induced kidney tissues. Relative mRNA expression levels of IL-1 $\beta$ , IL-6, TNF- $\alpha$  and IL-10 in kidney tissues from the three groups after 4 weeks of treatment. Data are presented as the mean  $\pm$  SEM; n=6 per group. \*P<0.05. Lut, luteolin; AngII, angiotensin II.

that Lut reduced the AngII-induced increase in the expression levels of inflammatory molecules, including IL-1 $\beta$ , IL-6 and TNF- $\alpha$ . In addition, Lut decreased inflammatory cell infiltration in AngII-induced renal damage of ApoE<sup>-/-</sup> mice, as determined via H&E staining. Seelinger *et al* (31) reported similar results, suggesting that TNF- $\alpha$ , IL-1 $\beta$  and IL-6 were all targets of Lut. In acute ischemic renal failure, TNF- $\alpha$  is an upstream molecule of the inflammatory cascade, which can initiate the upregulation of cytokines and chemokines (32). IL-1 $\beta$  and IL-6 are downstream molecules in the inflammatory cascade, which can directly impair kidney function (32). Hashmat *et al* (33) revealed that IL-6 production may participate in the development of salt-sensitive hypertension and end-organ damage by mediating increased infiltration into the kidney. Furthermore, Hong *et al* (13) reported that Lut exhibited anti-inflammatory effects by inhibiting pro-inflammatory cytokine release. The results were consistent with those observed in the present study.

The mechanism of autophagy has been investigated in detail due to its involvement in several diseases, including tumorigenesis, cardiomyopathy, diabetes, fatty liver, pulmonary, neurodegenerative and kidney diseases (34-39). In the present study, autophagy participated in AngII-induced renal damage of ApoE<sup>-/-</sup> mice. LC3 and p62 are central autophagy-related proteins involved in the autophagic flux (40). Autophagy is a dynamic cellular catabolic process accompanied by LC3-II conversion from LC3-I and p62 degradation (41). LC3-II is regarded as a promising autophagosome marker (42,43). p62 is a LC3-interacting protein that transports ubiquitinated protein aggregates to autophagosomes via its association with LC3-II (44). When autophagy is impaired, p62 expression is increased in cells and tissues (9). Schläfli *et al* (45) have demonstrated that high LC3 levels are associated with lower tumor aggressiveness, whereas p62 expression in general, is significantly associated with aggressive tumor behavior. Guan *et al* (10) reported that autophagy reduces the initiation of the apoptotic process in I/R mice with renal damage. The authors suggested that the levels of autophagy were increased earlier than the induction of apoptosis. This effect was noted after 2 h of reperfusion and reached its maximum level on day 2 (10). Subsequently, autophagy declined from day 3 when renal damage had been nearly recovered to normal levels (10). A consistent trend was noted in the present study. For instance, the p62 protein levels in the AngII + Lut group were downregulated compared with those noted in the AngII group, whereas LC3 protein levels in the AngII + Lut group were upregulated compared with those in the AngII group. Consistent results were obtained using immunostaining analysis. The data suggested that Lut protected against AngII-induced renal damage by inducing autophagy and inhibiting apoptosis.

In conclusion, the present study demonstrated that Lut treatment exhibited a protective effect on AngII-induced renal injury of ApoE<sup>-/-</sup> mice. This compound protected the kidney mainly by inhibiting collagen deposition and inflammation, while it could also induce autophagy. The findings of the present study may be used in the development of novel strategies for the prevention and treatment of renal damage. But, this study does not provide enough in-depth evidence, and thus further experiments and clinical research are needed to prove the effectiveness and safety of Lut.

## Acknowledgements

Not applicable.

## Funding

The present study was supported by a grant from the Dalian Medical Science Research Program of China (grant no. 1712009).

## Availability of data and materials

The datasets used and/or analyzed during the current study are available from the corresponding author on reasonable request.

## Authors' contributions

ZNG and HYL designed this study. YSL and QY aided in performing the experiments. XYL, LL and SL analyzed the data and interpreted the results of the experiments. ZNG and YSL confirm the authenticity of all the raw data. SL prepared the figures. QY drafted the manuscript. XYL and LL aided in the revisions of the manuscript. HYL provided the research funds. All authors read and approved the final manuscript.

## Ethics approval and consent to participate

All animal experiments were approved by the ethics committee of Dalian Municipal Central Hospital Affiliated to Dalian Medical University.

## Patient consent for publication

Not applicable.

## Competing interests

The authors declare that they have no competing interests.

## References

1. Umanath K and Lewis JB: Update on diabetic nephropathy: Core curriculum 2018. *Am J Kidney Dis* 71: 884-895, 2018.
2. Skov J, Christiansen JS and Poulsen PL: Hypertension and diabetic nephropathy. *Endocr Dev* 31: 97-107, 2016.
3. Sharma N, Malek V, Mulay SR and Gaikwad AB: Angiotensin II type 2 receptor and angiotensin-converting enzyme 2 mediate ischemic renal injury in diabetic and non-diabetic rats. *Life Sci* 235: 116796, 2019.
4. Urushihara M and Kagami S: Role of the intrarenal renin-angiotensin system in the progression of renal disease. *Pediatr Nephrol* 32: 1471-1479, 2017.
5. Kaliappan G, Nagarajan P, Moorthy R, Kalai Gana Selvi S, Avinash Raj T and Mahesh Kumar J: Ang II induce kidney damage by recruiting inflammatory cells and up regulates PPAR gamma and Renin 1 gene: Effect of  $\beta$  carotene on chronic renal damage. *J Thromb Thrombolysis* 36: 277-285, 2013.
6. Kelly TN, Raj D, Rahman M, Kretzler M, Kalleem RR, Ricardo AC, Rosas SE, Tao K, Xie D, Hamm LL, *et al*; CRIC Study Investigators: The role of renin-angiotensin-aldosterone system genes in the progression of chronic kidney disease: Findings from the Chronic Renal Insufficiency Cohort (CRIC) study. *Nephrol Dial Transplant* 30: 1711-1718, 2015.
7. Kuksal N, Chalker J and Mailloux RJ: Progress in understanding the molecular oxygen paradox - function of mitochondrial reactive oxygen species in cell signaling. *Biol Chem* 398: 1209-1227, 2017.

8. Liu Y, Shi B, Li Y and Zhang H: Protective Effect of Luteolin Against renal ischemia/reperfusion injury via modulation of pro-inflammatory cytokines, oxidative stress and apoptosis for possible benefit in kidney transplant. *Med Sci Monit* 23: 5720-5727, 2017.
9. Tanida I: Autophagy basics. *Microbiol Immunol* 55: 1-11, 2011.
10. Guan X, Qian Y, Shen Y, Zhang L, Du Y, Dai H, Qian J and Yan Y: Autophagy protects renal tubular cells against ischemia/reperfusion injury in a time-dependent manner. *Cell Physiol Biochem* 36: 285-298, 2015.
11. Imran M, Rauf A, Abu-Izneid T, Nadeem M, Shariati MA, Khan IA, Imran A, Erdogan Orhan I, Rizwan M, Atif M, *et al*: Corrigendum to 'Luteolin, a flavonoid, as an anticancer agent: A review' [Biomed. Pharmacother. 112 (2019) 108612]. *Biomed Pharmacother* 116: 109084, 2019.
12. Luo Y, Shang P and Li D: Luteolin: A flavonoid that has multiple cardio-protective effects and its molecular mechanisms. *Front Pharmacol* 8: 692, 2017.
13. Hong X, Zhao X, Wang G, Zhang Z, Pei H and Liu Z: Luteolin treatment protects against renal ischemia-reperfusion injury in rats. *Mediators Inflamm* 2017: 9783893, 2017.
14. Xin SB, Yan H, Ma J, Sun Q and Shen L: Protective effects of luteolin on lipopolysaccharide-induced acute renal injury in mice. *Med Sci Monit* 22: 5173-5180, 2016.
15. Sung J and Lee J: Anti-inflammatory activity of Butein and Luteolin through suppression of NFκB activation and induction of heme oxygenase-1. *J Med Food* 18: 557-564, 2015.
16. Choi JS, Islam MN, Ali MY, Kim YM, Park HJ, Sohn HS and Jung HA: The effects of C-glycosylation of luteolin on its antioxidant, anti-Alzheimer's disease, anti-diabetic, and anti-inflammatory activities. *Arch Pharm Res* 37: 1354-1363, 2014.
17. Seelinger G, Merfort I, Wölfle U and Schempp CM: Anti-carcinogenic effects of the flavonoid luteolin. *Molecules* 13: 2628-2651, 2008.
18. Domitrović R, Cvijanović O, Pugel EP, Zagorac GB, Mahmutefendić H and Škoda M: Luteolin ameliorates cisplatin-induced nephrotoxicity in mice through inhibition of platinum accumulation, inflammation and apoptosis in the kidney. *Toxicology* 310: 115-123, 2013.
19. Kang KP, Park SK, Kim DH, Sung MJ, Jung YJ, Lee AS, Lee JE, Ramkumar KM, Lee S, Park MH, *et al*: Luteolin ameliorates cisplatin-induced acute kidney injury in mice by regulation of p53-dependent renal tubular apoptosis. *Nephrol Dial Transplant* 26: 814-822, 2011.
20. Honjo T, Chyu KY, Dimayuga PC, Lio WM, Yano J, Trinidad P, Zhao X, Zhou J, Cercsek B and Shah PK: Immunization with an ApoB-100 related peptide vaccine attenuates angiotensin-II induced hypertension and renal fibrosis in mice. *PLoS One* 10: e0131731, 2015.
21. Cha J, Ivanov V, Ivanova S, Kalinovsky T, Rath M and Niedzwiecki A: Evolution of angiotensin II-mediated atherosclerosis in ApoE KO mice. *Mol Med Rep* 3: 565-570, 2010.
22. Xu Y, Zhang J, Liu J, Sai Li, Cheng Li, Wang W, Ma R and Liu Y: Luteolin attenuate the D-galactose-induced renal damage by attenuation of oxidative stress and inflammation. *Nat Prod Res* 29: 1078-1082, 2015.
23. Zhang W, Wang W, Yu H, Zhang Y, Dai Y, Ning C, Tao L, Sun H, Kellems RE, Blackburn MR, *et al*: Interleukin 6 underlies angiotensin II-induced hypertension and chronic renal damage. *Hypertension* 59: 136-144, 2012.
24. Zhong J, Guo D, Chen CB, Wang W, Schuster M, Loibner H, Penninger JM, Scholey JW, Kassiri Z and Oudit GY: Prevention of angiotensin II-mediated renal oxidative stress, inflammation, and fibrosis by angiotensin-converting enzyme 2. *Hypertension* 57: 314-322, 2011.
25. National Research Council (US): Committee for the Update of the Guide for the Care and Use of Laboratory Animals. 8th edition. National Academies Press, Washington, DC, 2011.
26. Shingu C, Koga H, Hagiwara S, Matsumoto S, Goto K, Yokoi I and Noguchi T: Hydrogen-rich saline solution attenuates renal ischemia-reperfusion injury. *J Anesth* 24: 569-574, 2010.
27. Livak KJ and Schmittgen TD: Analysis of relative gene expression data using real-time quantitative PCR and the 2(-Delta Delta C(T)) method. *Methods* 25: 402-408, 2001.
28. Domitrović R, Jakovac H, Tomac J and Sain I: Liver fibrosis in mice induced by carbon tetrachloride and its reversion by luteolin. *Toxicol Appl Pharmacol* 241: 311-321, 2009.
29. Chen CY, Peng WH, Wu LC, Wu CC and Hsu SL: Luteolin ameliorates experimental lung fibrosis both in vivo and in vitro: Implications for therapy of lung fibrosis. *J Agric Food Chem* 58: 11653-11661, 2010.
30. Chen J, Shetty S, Zhang P, Gao R, Hu Y, Wang S, Li Z and Fu J: Aspirin-triggered resolvin D1 down-regulates inflammatory responses and protects against endotoxin-induced acute kidney injury. *Toxicol Appl Pharmacol* 271: 118-123, 2014.
31. Seelinger G, Merfort I and Schempp CM: Anti-oxidant, anti-inflammatory and anti-allergic activities of luteolin. *Planta Med* 74: 1667-1677, 2008.
32. Okusa MD: The inflammatory cascade in acute ischemic renal failure. *Nephron* 90: 133-138, 2002.
33. Hashmat S, Rudemiller N, Lund H, Abais-Battad JM, Van Why S and Mattson DL: Interleukin-6 inhibition attenuates hypertension and associated renal damage in Dahl salt-sensitive rats. *Am J Physiol Renal Physiol* 311: F555-F561, 2016.
34. Levine B, Kroemer G: Autophagy in the pathogenesis of disease. *Cell* 132: 27-42, 2008.
35. Corrochano S, Renna M, Tomas-Zapico C, Brown SD, Lucas JJ, Rubinsztein DC and Acevedo-Arozena A: α-synuclein levels affect autophagosome numbers in vivo and modulate Huntington disease pathology. *Autophagy* 8: 431-432, 2012.
36. Eskelinen EL and Saftig P: Autophagy: A lysosomal degradation pathway with a central role in health and disease. *Biochim Biophys Acta* 1793: 664-673, 2009.
37. Virgin HW and Levine B: Autophagy genes in immunity. *Nat Immunol* 10: 461-470, 2009.
38. Luciani A, Vilella VR, Esposito S, Brunetti-Pierri N, Medina D, Settembre C, Gavina M, Pulze L, Giardino I, Pettoello-Mantovani M, *et al*: Defective CFTR induces aggresome formation and lung inflammation in cystic fibrosis through ROS-mediated autophagy inhibition. *Nat Cell Biol* 12: 863-875, 2010.
39. He L, Livingston MJ and Dong Z: Autophagy in acute kidney injury and repair. *Nephron Clin Pract* 127: 56-60, 2014.
40. Schmitz KJ, Ademi C, Bertram S, Schmid KW and Baba HA: Prognostic relevance of autophagy-related markers LC3, p62/sequestosome 1, Beclin-1 and ULK1 in colorectal cancer patients with respect to KRAS mutational status. *World J Surg Oncol* 14: 189, 2016.
41. Lee YK, Jun YW, Choi HE, Huh YH, Kaang BK, Jang DJ and Lee JA: Development of LC3/GABARAP sensors containing a LIR and a hydrophobic domain to monitor autophagy. *EMBO J* 36: 1100-1116, 2017.
42. Schläfli AM, Berezowska S, Adams O, Langer R and Tschan MP: Reliable LC3 and p62 autophagy marker detection in formalin fixed paraffin embedded human tissue by immunohistochemistry. *Eur J Histochem* 59: 2481, 2015.
43. Kabeya Y, Mizushima N, Ueno T, Yamamoto A, Kirisako T, Noda T, Kominami E, Ohsumi Y and Yoshimori T: LC3, a mammalian homologue of yeast Apg8p, is localized in autophagosome membranes after processing. *EMBO J* 19: 5720-5728, 2000.
44. Jin Z, Li Y, Pitti R, Lawrence D, Pham VC, Lill JR and Ashkenazi A: Cullin3-based polyubiquitination and p62-dependent aggregation of caspase-8 mediate extrinsic apoptosis signaling. *Cell* 137: 721-735, 2009.
45. Schläfli AM, Adams O, Galván JA, Gugger M, Savic S, Bubendorf L, Schmid RA, Becker KF, Tschan MP, Langer R, *et al*: Prognostic value of the autophagy markers LC3 and p62/SQSTM1 in early-stage non-small cell lung cancer. *Oncotarget* 7: 39544-39555, 2016.



This work is licensed under a Creative Commons Attribution-NonCommercial-NoDerivatives 4.0 International (CC BY-NC-ND 4.0) License.